Review Article

Application of Iron Oxide Nanomaterials for the Removal of Heavy Metals

Pragnesh N. Dave[1] **and Lakhan V. Chopda**[2]

[1] *Department of Chemistry, Krantiguru Shyamji Krishna Verma Kachchh University, Mundra Road, Bhuj, Gujarat 370 001, India*
[2] *Chemical Engineering Department, Government Engineering College, Bhuj, Gujarat 370 001, India*

Correspondence should be addressed to Pragnesh N. Dave; pragnesh7@yahoo.com

In the 21st century water polluted by heavy metal is one of the environment problems. Various methods for removal of the heavy metal ions from the water have extensively been studied. Application of iron oxide nanaparticles based nanomaterials for removal of heavy metals is well-known adsorbents for remediation of water. Due to its important physiochemical property, inexpensive method and easy regeneration in the presence of external magnetic field make them more attractive toward water purification. Surface modification strategy of iron oxide nanoparticles is also used for the remediation of water increases the efficiency of iron oxide for the removal of the heavy metal ions from the aqueous system.

1. Introduction

Water is the most essential compound on the earth for the human activities. Proving clean water is the prime requirement of the human being for their better health. Water pollution is increasing worldwide due to rapid growth of industry, increase human population, and domestic and agricultural activities which leads to the life time threatening diseases [1]. Heavy metals pollution is becoming one of the most serious environment problems globally [2–5]. It is the most threat problem for population in dense countries particularly for China and India [6–10]. Its presence in low concentration of heavy metals in various water resources could be harmful to human health. The treatment of heavy metals is so important due to their persistence in the environment. In order to detoxify heavy metals, various techniques like photocatalytical oxidation, chemical coagulants, electrochemical, bioremediation, ion-exchange resins, reverse osmosis, and adsorption have been employed [11, 12]. Among these nano-based adsorbents are the more convenient technologies for removal of heavy metals from the aqueous system [13–16]. Application of iron oxide based nanomaterial is more attractive for removal of heavy metals

contamination from the water because of their important features like small size, high surface area, and magnetic property [17–22]. Magnetic property of iron oxide nanaparticles enables easy separation of adsorbents from the system and could be reused for further application. Reusability of iron oxide based nanomaterial leads to a decrease in the economic burden. Here in, we will provide detail account on iron oxides nanaparticles such as magnetite (Fe_3O_4), maghemite (γ-Fe_2O_3), and hematite (α-Fe_2O_3) based nanoadsorbents for removal of heavy metals from water/wastewater. We will put more emphasis on magnetite based nanoadsorbents.

2. Iron Oxide Nanoparticles

The synthesis of the above iron oxide nanoparticles is intensively developed not only for their fundamental scientific interest but their important application in various fields. Recently utilization of iron oxide based nanomaterials with novel property and functionality is widely studied due to their small size, high surface area, and magneti property [23, 24]. Synthesis of iron oxide nanoparticles has been extensively reviewed [23–26]. Iron oxide nanoparticles are synthesized
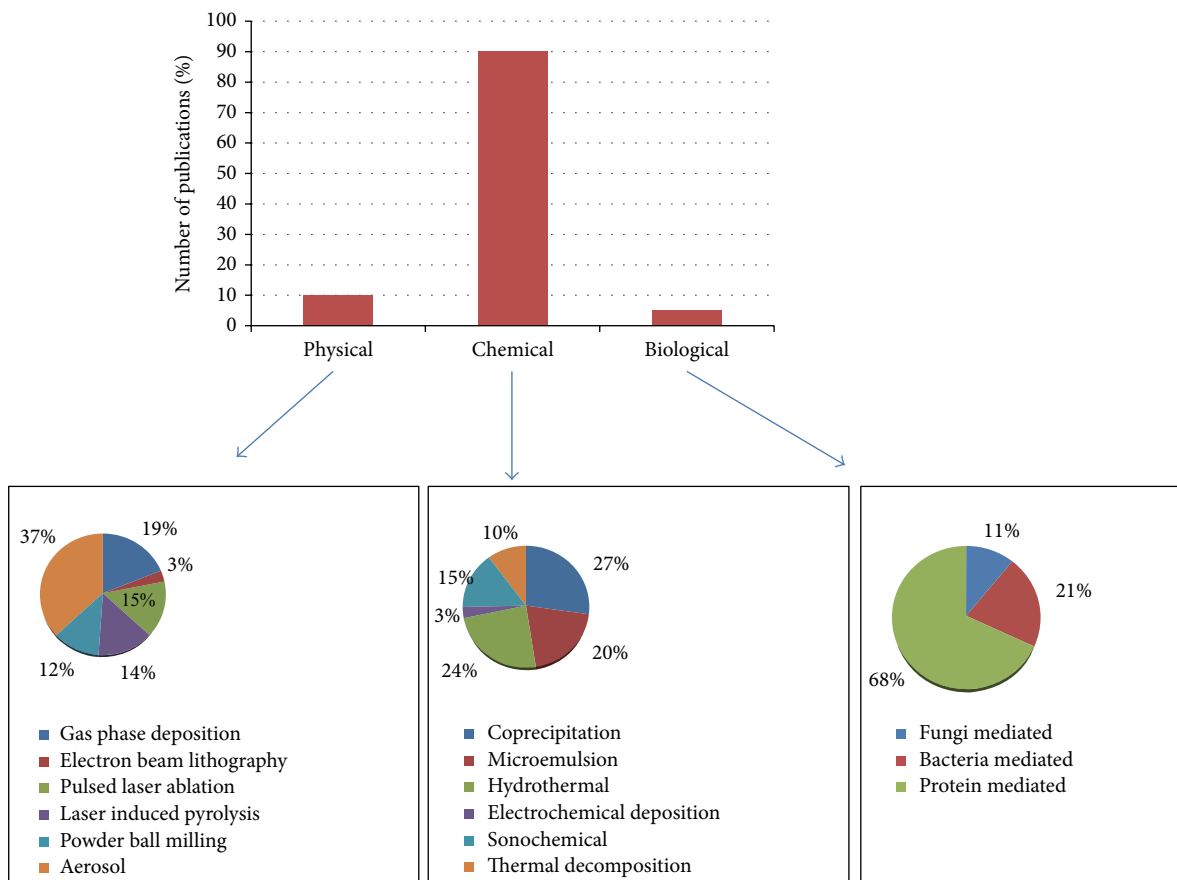
FIGURE 1: Synthesis of iron oxide nanoparticles by three different methods (adapted from [26]).

by three important methods such as physical, chemical, and biological as represented in the Figure 1. Chemical methods are well known and widely accepted methods for bulk production of iron oxide nanaparticles. There are many chemical methods such as chemical co-precipitation, thermal decomposition, sol-gel, electrochemical that have been reported in the literature which are shown in the Figure 1. Discussion of all synthetic methodologies in detail is the out of scope of this review. Concise overviews about synthetic methodology of IONPs are described here. Chemical coprecipitation method is a widely applicable method for synthesis of IONPs [27]. The chemical coprecipitation method involves the stoichiometric mixture of ferrous and ferric salts in ratio 2 : 1 (Fe^{3+}/Fe^{2+}) in aqueous medium in the presence of base and absence of oxygen. Formation of Fe_3O_4 is shown in (1) which is complete at a pH between 8 and 14. In the presence of oxygen and acid magnetite nanoparticles are converted into magnetite nanoparticles. The main advantage of this approach is that it produces a large amount of material, with control over particle size (2–20 nm) and shape afforded by adjusting pH, ionic strength, and the concentration of solution. In the thermal decomposition method iron oleate can be performed from the decomposition of the iron precursor such as $Fe(Cup)_3$, $Fe(CO)_5$, and $Fe(acac)_3$ in the organic solvent and surfactants at high temperature. The main advantage of thermal decomposition method is that, it improves control over the size and

shape of iron oxides nanoparticles. The size and shape of iron oxides nanoparticles depend on the precursor and temperature [28, 29]. Hydrothermal involves iron precursors in water by applying high pressure and temperature. The reactions are carried out in the reactors or autoclaves. In hydrothermal condition, nanoparticles were formed by hydrolysis and oxidation followed by neutralization of mixed metal hydroxides. Ferromagnetic Fe_3O_4 NPs with diameter of 27 nm have been synthesized by a hydrothermal route in the presence of a surfactant sodium bis(2-ethylhexyl)sulfosuccinate [30]. Aqueous ferrofluid iron oxides nanoparticles synthesized by hydrothermal method using citric acid as reducing agent. The particles size are about 8 nm [31]. Surface modification of IONPs by polyethyleneimine was also prepared by hydrothermal method [32]. Others methods to prepare iron oxide nanoparticles are described in Table 1.

Consider

$$Fe^{+2} + 2Fe^{+3} + 8OH^- \longrightarrow Fe_3O_4. \tag{1}$$
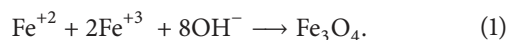
To understand the behavior of colloidal ferrofluid particles and improve their application carefully studied related to their fluid stability are necessary. Iron oxide nanoparticles are easily subject to aggregation in aqueous system and biological system. IONPs exhibit the hydrophilic surface due to presence of hydroxyl groups. There is hydrophilic interaction between particles and these particles form the

TABLE 1: Various chemical methods for synthesis of iron oxide nanoparticles.

| Name of method	Preparation method	Advantage	References
Microemulsion	Iron salt and base solution are mixed together which disperse in oil phase by adding surfactant	Diversity of iron oxide nanoparticles is prepared by varying the nature and concentration surfactant and reaction condition	[45–47]
Polyols method	Iron salt solvent dissolves in the polyols solvent. The suspension is stirred and heats up to boiling point of solvent. Polyols act as reducing as well as stabilizer	Control of particle growth and prevention of interparticle aggregation and obtaining well-defined shape and control size of particles	[48–50]
Sonolysis	Organometallic precursors decomposed by sonolysis	High magnetization and crystallinity achievement	[51–53]
Gas-aerosol	Ferric salts and a reducing agent in organic solvent are sprayed into a series of reactors and aerosol solute condenses and evaporation of solvent	Different size and shape of particles were prepared by using different iron precursors	[54–56]
Sol-gel	Hydroxylation and condensation of molecular precursors in solution are known as "sol," while evaporation of solvent to form three-dimensional network of nanoparticles is called "gel"	Control of particles size and stability of particles in sol-gel matrix	[57]
Electrochemical decomposition	Iron oxide nanoparticles produce by oxidation of iron electrode in aqueous solution	Particles size control by adjusting current density	[58–60]
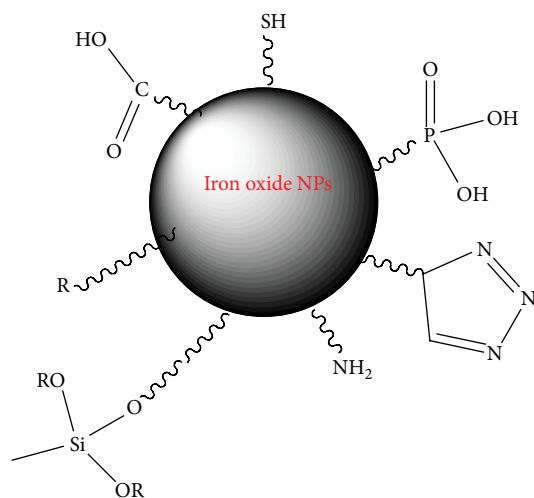
FIGURE 2: Schematic representation of surface modification of iron oxide nanoparticles.

agglomerate and resulted in large clusters. For stability among nanoparticles there is balance between attractive and repulsive force acting between nanoparticles [24]. To overcome this problem, there is requirement of electronic and steric stability of IONPs. Presence of hydroxyl groups on the surface of IONPs provides a versatile synthetic tool to attach different functionalities. Surface modification methodologies of IONPs improved the stability and provide novel proprieties to materials. The stabilization of the iron oxide particles is so important to produce magnetic colloidal "ferrofluids." These ferrofluids are stable against aqueous, biological medium and magnetic field. Modified magnetic nanoparticles have numerous applications in biomedical such as drug delivery, magnetic resonance imaging, hyperthermia, cellular labeling,

protein separation, and remediation of environment. There are different methodologies that have been reported for fabrication of INOPs as represented in Figure 2. Attachment of alkoxysilane to the surface of IONPs using different silane coupling agents is the most common surface modification technique. Organosilane is an attractive reagent for surface modification of nanoparticles because of an easy commercial availability, a simple synthetic method to immobilize on the surface of nanoparticles, and providing variety of functionality. Si-OR group of silane react with surface hydroxyl group of IONPs [33–35]. It is the hydrolysis and condensation reaction. By using trialkoxy silane functional group help to introduce various functionality such as amine, azide, aldehyde, thio, halide, hydroxyl, and acid on the surface of IONPs. Silane coupling agent further provides versatile tools to attach small organic molecules, polymers, and biomolecules to the surface. INOPs surface modifies by PEG using APS [36]. Molecular weight of PEG more than 1000 gm/mL formed the stable nanoparticles. Magnetic nanoparticles are coated with silane-PEG. Oleic acid on the surface of IONPs replaced by biocompatible silane PEG polymer for magnetic resonance imaging of murine tumors [37]. Ahangaran et al. reported the surface modification of magnetic nanaparticles by coating of silica. The hydrophilic nature of nanoparticles easily aggregate. Vinyltriethoxysilane acts as a coupling agent which provides hydrophobicity to the surface and decrease the agglomerations [38]. Immobilization of cyanoethyl triethoxysilane on the surface of Fe_3O_4. Cyano group on the surface stabilizes the magnetite nanoparticles and also improves the cellular labeling and the cell targeting [39]. Click chemistry is also an important method to modify INOPs. Click reaction such as azide-alkyne, thio-ene, thio-yne, and diels-alder is used for modification of the surface of magnetic nanoparticles. Oligonucleotides immobilized on the surface of SPINOs. There is azide-alkyne copper that mediates click reaction between oligonuclotides bearing alkyne with using alkyne

NHS-ester reagent and azide functional group on the surface of SPINOs. These nanoparticles can easily cross the HeLa cell membranes without using transfection agents as compared to their Au analogues [40]. Surface of SPINOs modifies by copolymers of poly(glycidyl methacrylate-co-poly(ethylene glycol) methyl ether methacrylate using atom transfer-free radical polymerization (ATRP) and introduces folic acid (FA) via azide-alkyne click reaction and they stabilize in the water so as to prolong *in vivo* circulation time [41]. SPIONs-P(GMA-co-PEGMA)-FA prepared by combination of ATRP and click chemistry can potentially be a good candidate for enhancing the targeting efficiency of cancer cells [42]. SPIONs-loaded cisplatin an anticancer drug conjugated to amphiphilic poly(ε-caprolactone)-*b*-poly-(propargyl methacrylate-click-mercaptosuccinic acid-co-poly-(ethylene glycol) methyl ether methacrylate) (PCL-*b*-P-(PMA-click-MSA-co-PEGMA) was synthesized by a combination of ROP, RAFT polymerization and thiol-yne click chemistry [43]. These are potential drug delivery systems of cisplatin for bladder cancer therapy. Hyper branch polyethylene glycol attached to surface of magnetic nanoparticles by using thio-ene click reaction is useful for active targeting anticancer agents [44].

3. Arsenic Removal by Using Iron Oxide Nanaparticles and Their Nanomaterials

Water contamination by arsenic salt is one of the big environmental pollution. It causes life time diseases such as cancer, neurological disorder, nausea, hyperkeratosis, muscular weakness, and many others [74]. Arsenic contamination in drinking water has been found domestically which can be led to numerous diseases. It was reported by world health organization in 2006 that around 45–57 million people in Bangladesh and 13 million people in United States have been exposed to unsafe arsenic contaminated water [75]. As per guide lines of USEPA, maximum contaminant level of arsenic in the drinking water should be 0.010 ppm [76]. It is therefore necessary to have an effective method to remove arsenic from the natural water and waste water. Iron oxides nanoparticles have shown prominent result for decontamination of arsenic from the water [77–79]. So they could become cost-effective materials for decontamination of arsenic from the water. Magnetite, hematite, and maghemite nanoparticles are synthesized by various chemical methods to remove As(III) and As(V) from water as presented in Table 2. The small size and high surface area of magnetite nanoparticles make them and ideal adsorbent. Heavy metals in the solution easily diffuse on the active surface of Fe_3O_4 nanoparticles. Surface area of magnetic nanoparticles plays a significant role in the adsorption process. The high surface nanoparticles can easily undergo aggregation in the solution which could decrease their efficiency so it is important to modify the surface of IONPs for improving their activity. Surface of iron oxides nanoparticles can be modified by the attachment with suitable functional groups such as carboxylic acids, phosphoric acid, silanol, thio, and amine as well as small organic molecules, biomolecules,

polymer, and other metal nanoparticles as represented in Figure 2. Feng et al. synthesized supermagnetic ascorbic acid-coated Fe_3O_4 by hydrothermal method. These nanocomposites have a diameter less than 10 nm and surface area about 179 m^2/g. The ascorbic acid-coated Fe_3O_4 shows super paramagnetic property at room temperature and saturation magnetization approaches 40 emug^{-1} and they are employed as an adsorbent to remove arsenic from the waste water. The maximum adsorption capacity of As(V) and As(III) is 16.56 mg/g, and 46.06 mg/g, respectively, as followed by Langmuir isotherm [80]. Formation of Fe_2O_3 nanoparticles in the matrix of cellulose has been reported by one pot chemical co-precipitation method [81]. The surface area of these nanocomposites is 113 m^2/g. They are demonstrated for the removal of arsenic from aqueous solution. They showed excellent adsorption capacity to remove As(III) and As(V) 23.16, 32.11, 9.64, and 3.25 mg/g followed by Langmuir and Freundlich isotherm, respectively. β-Cyclodextrin (CMβCD)-monodisperse magnetite nanoparticles with average nanoparticles size 10 nm are prepared by thermal decomposition and postgrafting methodology [82]. These CMCD-Fe_3O_4 are used to remediate of As(III), As(V), 2-naphthol, and naphthalene. Fe_2O_3 chestnut-like amorphous-core/γ-phase shell hierarchical nanostructure that showed the strong adsorption of As(V). It adsorbed 143.12 m^2/g of As(V) [83]. There are numerous applications of magnetic nanomaterial to remove arsenic salts from water that are summarized in Table 3.

4. Removal of Copper and Chromium and Chromium Metal

Copper has enormous application in the industry. It is used in the electroplating, paint and pigment industry, electrical, and fertilizer. Due to wide range of application of copper can be accumulated in the environment which makes water more pollute. Surface modification of magnetite nanoparticles is by ligand 1; 6hexadiamine has been reported [84]. This is useful for removal of Cu(II) from aqueous system. Magnetic nanoparticles bearing amine group on their surface were able to remove 98% copper from polluted river and tap water. The equilibrium is achieved within five minutes and kinetics followed the pseudosecond order mechanism. The maximum adsorption capacity was 25.77 mg/g at pH 6 and 298 K. Amine functional group also immobilized on the surface of silica coated magnetic nanoparticles by 3-aminopropyltriethoxysilan using sol-gel method. The adsorption capacity of magnetic nanoparticles that exhibit amine group is 22.4 mg/g [85]. In the above case magnetic nanoparticles having amine functionality on the surface lead to an increase in adsorption capacity which increases with pH. At lower pH, amine group undergoes protonation which decreases adsorption efficiency; however, at higher pH strong complexation takes place between Cu^{+2} and free amine group. Banerjee and Chen reported Fe_3O_4-gum-arabic nanocomposite for removal of Cu(II). Gum arabic attach to surface of Fe_3O_4 via coupling between surface hydroxyl group

TABLE 2: Application of iron oxides nanaparticles for removal of arsenic according to the Langmuir isotherm.

Name of IONPs	Method of synthesis	Size (nm)	BET surface area m^2/g	Sorption capacity of As (III) mg/g	Sorption capacity of As (V) mg/g	References
γ-Fe$_2$O$_3$	Chemical coprecipitation	7–12	168.73	67.02 (30°C)	95.37 (350°C)	[61]
Fe$_3$O$_4$	Chemical coprecipitation	17	—	8.2[a] and 5.68[b]	6.71[a] and 4.78[b]	[62]
α-Fe$_2$O$_3$	Chemical coprecipitation	12	—	1.25[a] and 20[b]	4.6[a] and 4.9[b]	[62]
α-Fe$_2$O$_3$	Solvent thermal	5	162	95	47	[63]
γ-Fe$_2$O$_3$	Wet chemical	4	100	—	45	[64]
Magnetite (55.8%) and Maghemite (44.2%)	Iron wires	34	12	2.9	3.05	[65]

[a]1 h contact time, [b]24 h contact time.

TABLE 3: Overview of various iron oxide nanomaterials for removal of arsenic.

Adsorbents	BET surface area (m^2/g)	Adsorption capacity (mg/g)		References
		As (III)	As (V)	
Magnetite-silica	163.54	—	170	[66]
MnFe$_2$O$_4$	138	93.8	90.4	[67]
CoFe$_2$O$_4$	101	100.3	73.8	[67]
Magnetic-graphene	148	13.10	5.83	[68]
Fe$_3$O$_4$-BC cellulose		—	36.9	[69]
Mesoporous Fe$_2$O$_3$@C	877	29.4	17.9	[70]
Magnetic binary oxide nanoparticles	123.8	23.25	—	[71]
Fe$_3$O$_4$ wheat saw		3.9	8.06	[72]
MI/CNTs	662.1	8.13	9.74	[73]

of nanoparticles and carboxylic acid group of GA. The average diameter of particles are in range of 13–67 nm and 5.1 wt% of arabic gum was immobilized. The adsorption rate is so fast and equilibrium was achieved within 2 min. It showed that chemical adsorption takes place and strong complexation between Cu(II) and amine group of arabic gum. The zeta potential value increased with decrease in pH of solution due to protonation of hydroxyl group of nanoparticles and carboxylic acid and amine of GA. The effect of pH on adsorption is also investigated at pH < 2 no adsorption took place. At pH 2–6 adsorption increases with increase in pH. The adsorption capacity of magnetic nanoparticles and GA-MNP is 17.6 and 38.5 mg/g, respectively, which is followed Langmuir isotherm. GA-MNP regenerated by using acid solution. The GA-MNP exhibits good reusability. The adsorption capacity of GA-MNP was 28.12, 27.64, and 27.18 mg/g in first, second, and third adsorption-desorption cycles, respectively [86]. Chitosan coated maghemite nanoparticles were modified with a biodegradable and ecofriendly reagent α-ketoglutaric acid and demonstrated for removal of Cu(II) from water [87]. These magnetic based nanoadsorbents were also characterized by XRD, FT-TR, TEM, VSM, and EDS. The particles size of CCMNPs bearing α-ketoglutaric acid is about 30 nm. In FT-IR spectra characteristic peak around 589 cm^{-1} indicates successful coating of γ-Fe$_2$O$_3$. Another characteristic peak of magnetic CCMNPs around 1644 cm^{-1} shows vibration of primary amine which disappears after

immobilization of α-ketoglutaric acid and new peak around 1618 cm^{-1} is the vibration peak of secondary amine that also confirmed coating of α-ketoglutaric acid to magnetic CCMNPs. The other bands are 1402 cm^{-1} and 1718 cm^{-1} of C–H stretching vibration of CH$_2$ from α-ketoglutaric acid and amide functional group, respectively. γ-Fe$_2$O$_3$ confirmed from XRD pattern. XRD becomes broader and lower indicating that KA modifies uniformly CCMNPs. The saturation magnetization of KA-CCMNPs is 33.5 emu/g which showed that they are super magnetic in nature and very susceptible to the external magnetic field. The adsorption data showed following Langmuir isotherm and maximum capacity of Cu(II) removal were 96.15 mg/g. Chitosan supported on the surface of magnetite nanoparticles. First chitosan carboxymethylated was prepared after that it was covalently attached to the Fe$_3$O$_4$ nanoparticles surface. They were employed for removal of Cu(II). The maximum adsorption capacity is 21.5 mg/g which followed Langmuir equation. The effect of pH and temperature was also demonstrated. The adsorption capacity increases with increase in pH [88]. Magnetic composite microspheres bearing of Fe$_3$O$_4$ nanoparticles and polyacrylic acid-chitosan were prepared by chemical coprecipitation method as an efficient adsorbent for removal of Cu(II) [89]. The CS/PPA-Fe$_3$O$_4$ microspheres have been exhibited higher adsorption capacity than CS-Fe$_3$O$_4$ microspheres. The Fe$_3$O$_4$-polyvinyl acetate-iminodiacetic acid contains EDTA and was also useful adsorbent for removal

of Cu(II) [90]. Carboxymethyl-β-cyclodextrin modified with magnetite nanoparticles (CMβCD-Fe$_3$O$_4$) are the efficient magnetic adsorbents for the detoxification of copper ions from the water. CMβCD grafted on the surface of magnetic nanoparticles by carbodiimide method. The high efficiency of this magnetic adsorbent is due to presence of multiple hydroxy and carboxyl groups. The adsorption of Cu(II) onto CMβCD-MNPs was found to be dependent on pH and temperature [91]. Magnetic-grapheme nanocomposites are reported by one pot thermal decomposition method. It is an efficient nanomaterial for removal of Cr(VI) from the waste water at low pH that it removed Cr(VI). The large saturation magnetization (96.3 emu/g) of the synthesized nanoparticles allows fast separation of the adsorbent. Recycling process is more energetically and economically sustainable. The significantly reduced treatment time required to remove the Cr(VI) and the applicability in treating the solutions with low pH makes magnetic-graphene adsorbent promising for the efficient removal of heavy metals [92]. Montmorillonite supported Fe$_3$O$_4$ nanoparticles exhibited good adsorption capacity than Fe$_3$O$_4$ for removal of Cr(VI) [93]. The high efficiency is due to montmorillonite possessed porosity which provides better dispersion of magnetite nanaparticles inside and less aggregation. The Magnetic nanaparticles supported on organ peel pith by using redox precipitation method. These nanaparticles have the 20 × 80 nm tubular shapes and octahedral crystals around 20–40 nm. It showed higher adsorption capacity than unmodified magnetic nanaparticles towards the removal of Cr(VI) [94]. Magnetite-polypyrrole composite microspheres have been synthesized using Fe$_3$O$_4$ microspheres as a chemical template under sonication. Fe$_3$O$_4$/PPy have a strong adsorption capacity for Cr(VI) with a maximum adsorption capacity of about 209.2 mg/g [95].

5. Removal of Other Heavy Metals

Fe$_3$O$_4$ nanoadsorbents have been demonstrated for the removal of Pb(II) ions from aqueous solution using a batch-adsorption technique. The effect of temperature, pH, and coexisting ions on the adsorption of Pb(II) has been studied in detail. Adsorption equilibrium was achieved within 30 min. The amount of Pb(II) adsorbed increases with increasing temperature that indicates endothermic adsorption as well as there is no effect of coexisting cation on the adsorption. The adsorption equilibrium data followed the Langmuir and Freundlich adsorption isotherm models. The thermodynamics of Pb(II) adsorption onto the Fe$_3$O$_4$ nanoadsorbents suggest that the adsorption was spontaneous, endothermic, and physical in nature. The maximum adsorption capacity of Pb is 36 mg/g [96]. Maghemite (γ-Fe$_2$O$_3$) nanoparticles for the selective removal of toxic heavy metals from electroplating wastewater. The maghemite nanoparticles of 60 nm were synthesized using a co-precipitation process. It was characterized by XRD and EDX. The adsorption of Pb(II) attained equilibrium within 15 min. The adsorption of Pb(II) increases with increase in the pH [97]. MNPs-Ca-alginate coated with *Phanerochaete chrysosporium* adsorbed about 90% of Pb(II) after repeated

five cycles [98] and reactive blue-19 dye on the surface of magnetic nanaparticles also an efficient adsorbent for decontamination of Pb(II) [99]. Water soluble magnetite nanoparticles prepared by hydrothermal method with high solubility and stability showed high affinity for Pb(II) and Cr(VI) than water insoluble magnetite nanoparticles [100]. This water soluble magnetic nanoparticles have the capacity to remove 90% of Pb(II) in 2 min. The high value of saturation magnetization (83.4 emu/g) can easily remove from the aqueous system. Flower- and hollow-like nest morphology of α-Fe$_2$O$_3$ nanoparticles was prepared by template-free solvent thermal method and glycerol mediated microwave-assisted methods [101, 102]. They were useful for removal of As(V) and Cr(V) from the water. The maximum adsorption capacity of 51 and 30 mg/g for the As(V) and Cr(V) on flower-like magnetic adsorbent, respectively, while 75.3 and 58.5 mg/g for the As(V) and Cr(V) on hollow nest-like magnetic adsorbent. Maghemite nanotubes were synthesized by microwave irradiation method. It was used as nanoadsorbent to detoxify heavy metals such as Cu(II), Zn(II), and Pb(II). The BET surface area was found to be 321.638 m^2/g and magnetic saturation was emu/g. From the Langmuir isotherms, the maximum adsorption capacities of tubular maghemite adsorbents towards Cu(II), Pb(II), and Zn(II) were 111.11, 71.42, and 84.95 mg/g, respectively. The kinetic data of adsorption of heavy metal ions on the synthesized nanoadsorbents were followed by a pseudosecond-order equation indicating their chemical adsorption [103]. Multiwall carbon nanotube-magnetite nanocomposites based magnetic nanoadsorbent were prepared. Thiol functional group was anchored on the surface of CNTs/Fe$_3$O$_4$ using 3-mercaptopropyltriethoxysilane [104]. The BET surface area of these adsorbent is 97.16 m^2/g. The maximum Langmuir adsorption capacity for removal of Pb and Hg(II) is 65.40 and 65.52 mg/g, respectively. Surface of Fe$_3$O$_4$ modified with 2-mercaptobenzthiazole is an efficient adsorbent for removal of toxic metal Hg(II) than unmodified magnetic nanoparticles. Unmodified nanaparticles are able to remove 43.47% of 50 ng/mL of Hg(II) from polluted water while modification with MBT improved the removal efficiency up to 98.6% in the same concentration within 4 min. There is no considerable effect on adsorption efficiency by variation of pH and electrolyte NaCl concentration [105]. Amine functionalize magnetite nanaparticles are useful adsorbent for decontamination of heavy metals such as lead, copper, and cadmium. AF-Fe$_3$O$_4$ prepared by hydrothermal method in which iron salt FeCl$_3$·6H$_2$O was added to ethylene glycol followed by sodium acetate and ethanediamine and sealed in teflon lined stainless-steel autoclave heat at 200°C temperature for 8 h. The morphology of AF-Fe$_3$O$_4$ was investigated by transmission electron microscopy. The mesoporous morphology has been observed in TEM picture. The pore volume and BET surface are 0.1833 cm^3/g and 25.94 m^2/g, respectively ray diffraction pattern proved that it is magnetite phase structure. The zeta-potential value decreased with increase of pH. The adsorption rate of AF-Fe$_3$O$_4$ follows pseudosecond-order kinetic model. The equilibrium was achieved within 120 min at pH 7. According to Langmuir

isotherm, the maximum adsorption capacity for Pb(II), Cd(II), and Cu(II) is 369, 446.4, and 523 mg/g, respectively. AF-Fe_3O_4 adsorbent is endothermic and spontaneous [106]. The surface functionalization of magnetic nanoparticles by copolymer of acrylic acid and crotonic acid which further modify with 3-aminopropyltroethoxysilane are the efficient adsorbent to detoxification of heavy metals such as Cu, Pb, Zn, and Cd(II) from the aqueous solution. The maximum adsorption capacities of these metals are 126.9, 166.1, 43.4, and 29.6 mg/g, respectively [107]. Humic acid coated magnetite nanaparticles were prepared by coprecipitation method. The saturation magnetization of 79.6 emu/g of Fe_3O_4-HA enables easy separation from the water at low magnetic field within a few minutes. The equilibrium reached in less than 15 min and Langmuir isotherm with maximum adsorption capacity was from 46.3 to 97.7 mg/g. They are stable in tap and natural water and acidic/basic solutions ranging from 0.1 M HCl to 2 M NaOH with leaching of Fe < 3.7% and humic acid < 5.3%. Fe_3O_4-HA was able to remove more than 99% of Hg and Pb(II) and 95% of Cu(II) and Cd(II) in natural and tap water [108]. Surface modifications of Fe_3O_4 with succinic acid, ethylenediamine, and 2,3-dimercaptosuccinic acid have been reported [109]. The TEM image of the above mentioned acid and thiol functional group supported to surface of Fe_3O_4 demonstrated formation of spherical nanaparticles with average sizes of carboxylic acid and thiol group are 10 nm and 6 nm, respectively, while amine functionalization shows the well-define and discrete morphology with mesoporous in nature. The average size of amine functionalize to magnetic nanoparticles is 40 nm and an average diameter is about of 6 nm. From the IR-spectra a strong vibration peak at $588 \, cm^{-1}$ in all three functionalized groups of magnetic nanoparticles assigned to stretching vibration of Fe–O. The band at 1690 and $1700 \, cm^{-1}$ is due to carbonyl stretching vibration of succinic acid (SA) and 2,3-dimercaptosuccinic acid (DMSA) which shifted at lower value at 1620 and $1660 \, cm^{-1}$ after being supported to magnetic nanoparticles and the same observation was also reported in the case of –NH_2 bending frequency in the spectra of ethylenediamine and amine-Fe_3O_4 spectra which confirms the immobilization of SA, DMSA, and EDA on the surface of magnetic nanoparticles. The pH of zero point charge of carboxyl-MNP and amine-MNP were found near about 4.5 and 4.7. The value of zeta potential of all three adsorbents is decreased with increase in pH; thus surface of carboxyl MNP and amine MNP have positive surface charge at pH $<$ pH_{pzc} and negative with pH $>$ pH_{pz}. The surface of thiol-MNP has negative surface charge in the range of pH 2–12. The mean hydrodynamic diameters were about 25 nm, 90 nm, and 17 nm for carboxyl, amine, and thiol MNP measured by DLS which indicated presence of hydrated organic layers. The carboxyl, amine and thiol groups are tightly bound on the surface of Fe_3O_4 which provide high stability in aqueous stability to magnetite nanoparticles. The saturation magnetization of carboxyl, thiol and amine MNP are found to be 59.5, 43.2, and 64.3 emu/g, respectively. Such strong magnetic property enables to separate of three adsorbents easily from the solution. These three adsorbents are demonstrated for

removal of heavy metals such as Cr(III), Ni(II), Co(II), Cu(II), Cd(II), Pb(II) and As(III). The removal efficiency increases with increase in the case that all three adsorbents are due to strong complexation that takes place between surface of adsorbents and metals ions and weak electrostatic interaction with surface. The adsorption capacities of all three adsorbents are increased with increasing of the concentration of adsorbents which proved that increase of more active sites on the surface. The removal adsorption of thiol-MNP is higher than carboxyl and amine. It can be explained on the basis of Pearson's hard soft acid base theory. The thiol is the soft Lewis base so that more interaction with soft Lewis acid such heavy metal ions. The removal efficiency decreases in the case of As(III) after increase in the pH because of As(III) hydrolyzed to $As(OH)_4^{-}$. The adsorption kinetic experiment was performed with amine-MNP which suggested that most of adsorption achieved within less than 15 minutes and pseudoequilibrium at 60 min. The adsorption takes place in two stages, a very fast and other very slow. The desorption experiment was performed using 10 mL 0.1 M HCl. All heavy metals were removed over to 85%. The removal efficiency gradually decreases after repeating three times. About 80% recovery could be achieved after three recycles. Surface of Fe_3O_4 with carboxy methyl-β-cyclodextrin (CMβCD) base magnetic nanoadsorbent selectively removes heavy metals such as of Pb(II), Cd(II), and Ni(II). The adsorption capacity of Pb(II), Cd(II), and Ni(II), 64.5, 27.7, and 13.2 mg/g, respectively [110]. Shellac is an natural biodegradable resin bearing hydroxyl and carboxyl group attached to Fe_3O_4 and demonstrated to remove Cd(II). The maximum adsorption capacity for removal of Cd(II) is 18.80 mg/g [111]. Superparamagnetic iron oxide nanaparticles surface was modified with dimercaptosuccinic acid (DMSA). They are demonstrated for removal of toxic metals such as a Hg, Ag, Pb, Cd, and Tl. The ligand DMSA effectively binds to metals. DMSA-Fe_3O_4 exhibited a capacity 227 mg/g of mercury which is a 30-fold larger value than conventional resin based sorbents (GT-73) [112]. The chemical affinity, capacity, kinetics, and stability of these adsorbents were compared with GT-73, activated carbon, and nonporous silica in ground water, river water, sea water, human blood, and plasma. The MNPs-DMSA were efficiently removed 99 wt% of 1 mg/L Pb within a minute. However other adsorbents such as GT-73 and chelex-100 took 120 and 10 min times to remove 96% of Pb.1, 6-Hexanediamine immobilized on the surface of Fe_3O_4. They are able to remove 98% of Pb(II) from the industrial water and tap water. The maximum adsorption capacity of Pb(II) is 40.10 mg/g by MNPs-NH_2 [113]. Magnetic nanoparticles were synthesized by three different methods such as coprecipitation, coprecipitation surface decoration, and polyol method [114]. The average particles sizes of all three methods are 8, 12, and 35 nm. These three are the important adsorbents for the removal of heavy metals such Ni(II), Cd(II), Cr(II), and Cu(II) from the waste water. The maximum adsorption capacities to detoxify heavy metals are 5.15, 7.45, and 35.46 mg/g, respectively. Fe_3O_4-NH_2/PEI-EDTA with an average diameter of 60 nm could be removed from multicomponent heavy metals such as Cu(II), Cd(II), and Pb(II). At pH near about 98% Pb(II) were

removed from the aqueous mixture [115]. Poly2-aminoethyl methacrylate hydrochloride polymer chain on Fe_3O_4 was followed by the transformation of pendant amino groups into dithiocarbamate (DTC) groups. This polymer-brush-based DTC-functionalized magnetic nanoadsorbent exhibits high chelating affinity toward Hg(II) and is able to remove complete mercury from the water. The author has also compared the capacity and efficiency of this adsorbent for removal of Hg(II) with its monolayer analogue that was prepared from direct transformation of amino groups of 3-aminopropyl triethoxysilane (APTEs) functionalize Fe_3O_4 to DTC functional group and other parameters such as adsorption thermodynamic, kinetics, and Langmuir and Freundlich isotherm which were also evaluated. The high surface functional group on Fe_3O_4-polyAEMA-DTC make it high efficiency adsorbent as compared to their monolayer analogues [116]. A novel CD/MWCNT-iron oxide composite was prepared by plasma-induced technique. They showed the high magnetic property and good dispersity in layer and also increased the adsorption capacity to detoxify the Zn(II) [117]. Hierarchical MnO_2-cated with magnetic nanocomposite (Fe_3O_4/MnO_2) was synthesized by hydrothermal process which showed the flower-like morphology. They are employed to remove heavy metal ions from the water. The high surface area and high magnetic saturation make them has good adsorption ability. The removal efficiency of Fe_3O_4/MnO_2 was compared with unmodified Fe_3O_4 nanoparticles for heavy metals such Cd(II), Cu(II), Pb(II), and Zn(II). According to Langmuir equilibrium sorption model, maximum adsorption capacity of Cd(II) was 53.2 mg/g. Fe_3O_4/MnO_2 retained over 80% of its adsorption capacity under various solution conditions that are typically encountered in natural waters. In presence of external magnetic field it was easily recovered and reused through consecutive adsorption-desorption experiments [118]. Near about 100% heavy metals were removed using Fe_3O_4-Zno magnetic semiconductor nanoparticles [119]. $MnFe_2O_4$@Mn-Co oxide based magnetic adsorbents have the maximum adsorption capacity to remove Pb(II), Cu(II), and Cd(II) were 481.2, 386.2, and 345.5 mg/g, respectively [120]. Polyacrylic acid covalently supported on the surface of Fe_3O_4 which further functionalize with amine group using diethylenetriamine. They are demonstrated for removal of Cu(II) and Cr(VI). The Langmuir isotherms for maximum adsorption capacity for both are 12.43 mg/g and 11.24 mg/g, respectively [121]. IONPs prepared by co-precipitation method followed by modification with 3-aminopropyltriethoxy silane and acrylic chloride which further grafted with polyacrylic acid. It is useful to removal of heavy metal such as Cd(II), Pb(II), Ni(II), and Cu(II) [122]. Magnetite nanorods with average diameter 60 nm were prepared by pulsed current electrochemical method. The implication of this nanorod for removal of heavy metals such as Fe(II), Zn(II), Cu(II), Pb(II), Ni(II), and Cd. The Langmuir maximum adsorptions of these metals are 127, 107.27, 79.10, 112.86, 95.42, and 88.38 mg/g, respectively [123].

6. Silica Based Magnetic Adsorbent for Removal of Heavy Metals

Silica coated magnetic nanoadsorbents provide stability and increase adsorption efficiency. Silica-modified magnetite NPs

functionalized with cetylpyridinium bromide complexation with 8-hydroxy quinoline used for detection of heavy metal ions such as Cd(II), Co(II), Cu(II), Mn(II), Ni(II), and Pb(II) from the water samples; however, detection limit of Cd(II), Co(II), Cu(II), Mn(II), Ni(II), and Pb(II) are 2.3, 9.5, 4.7, 15.3, 9.1, and 7.4, respectively in ng/L [124]. The porous magnetic spheres are prepared using Stöber and hydrothermal process and useful nanoadsorbent for detoxification of Ni(II) [125]. Wang et al. reported a novel amino functionalized Fe_3O_4@SiO_2 prepared by co-precipitation method [126] and characterized by XRD, VSM, TGA, zeta potential, and XPS. Amine functional group introduced by using silylation reagent 3-aminopropyltromethoxy silane. The BET surface area of Fe_3O_4, Fe_3O_4@SiO_2, and Fe_3O_4@SiO_2-NH_2 is 114, 318.5, and 216.2, respectively. The absorption peak at 565 cm^{-1} of Fe–O vibration. The adsorption bands at 1220, 1094, 804, and 471 cm^{-1} are the starching and deformation vibration of SiO_2 which indicate coating of SiO_2 on magnetic nanoparticles. It was further confirmed by others that observed absorption bands are 3361, 1572, 1498, and 692 cm^{-1} of stretching and bending vibration of amino group. XRD pattern at 30.4°, 35.6°, 43.3°, 57.3°, and 62.8° resulted in cubic spinel structure of Fe_3O_4 as well as same pattern also observed for Fe_3O_4@SiO_2 and Fe_3O_4@SiO_2-NH_2 showed stability of magnetic particles after coating SiO_2 layer. The particles size of Fe_3O_4, Fe_3O_4@SiO_2, and Fe_3O_4@SiO_2-NH_2 were 12.1, 13, and 13.4 nm calculated by using Scherrer equation respectively. The TEM image of three nanoparticles displayed core-shell structure with average particle sizes are 13.4, 16.6, and 18.4 nm, respectively. The saturation magnetization for Fe_3O_4, Fe_3O_4@SiO_2 and Fe_3O_4@SiO_2-NH_2 68, 36.2 and 34 emu/g, respectively, which indicate that all three nanaparticles are in superparamagnetic. Surface composition was measured by XPS in which result showed that $Fe_{2p3/2}$, Si_{2p2}, and N_{1s} are 2.73, 20.37 and 3.23 for Fe_3O_4@SiO_2-NH_2. The zeta potential was performed to measure surface charge. The values of zeta potential of Fe_3O_4@SiO_2 and Fe_3O_4@SiO_2-NH_2 were increased that indicated the stability of nanaparticles. The isoelectric point (IEP) of Fe_3O_4@SiO_2 and Fe_3O_4@SiO_2-NH_2 is 1.4 and 6 which showed the successful coating of silica layer and amine group on magnetite nanoparticles. The adsorption obeyed Langmuir isotherm equation. The adsorption capacities to remove heavy metals such as Cu(II), Pb(II), and Cd(II) at 25°C are 0.47, 0.37, and 0.20 mmol/g, respectively. The adsorption capacity increased with increasing temperature indicating endothermic nature of adsorption process. There is no drastic change on the adsorption of Cu(II) in the presence of humic acid but slightly decreased in adsorption capacity of Cu(II) in the presence of Na, K, and Mg because of competitive binding of these metals to adsorbent surface. Fe_3O_4@SiO_2-NH_2 exhibited good adsorption capacity after regeneration in the presence of acid. Fe_3O_4@SiO_2 prepared by using silica source Na_2SiO_3 and then modified with thiol group [127]. These showed high adsorption efficiency. They are able to remove 148.8 mg/g of mercury at pH 6.5 calculated from Langmuir isotherm equation. After recycling they showed 110 mg/g adsorption

TABLE 4: Pore diameter, pore volume, BET surface area, and adsorption capacity of SH-mSi@Fe$_3$O$_4$.

Pore volume (cm^3/g)	Pore diameter (nm)	Surface area BET (m^2/g)	Adsorption capacity (mg/g) (Langmuir isotherm equation)	
			Pb	Hg
0.29	2.5	321	91.5	260

capacity. Mesoporous silica nanoparticles based material such as MCM-41, MCM-48, and SBA-15 are one of the most important advanced materials. They have important features such as high surface area, definite pore size, and pore volume that make them ideal candidates for the remediation of water. Functionalization of such materials improved their physical and chemical properties and enhanced their adsorption capacity particularly for removal of pollutants. Multifunction microspheres with large pore sized mesoporous silica nanoparticles that contain Fe$_3$O$_4$ have been synthesized by sol-gel method using CTAB as surfactant [128]. They also modified amine functional group with using APTMS. Here CTAB first dissolved in water which resulted in Fe$_3$O$_4$@SiO$_2$@meso-SiO$_2$-R$_1$ while CTAB added directly to Fe$_3$O$_4$@SiO$_2$ called Fe$_3$O$_4$@SiO$_2$@meso-SiO$_2$-R$_2$. The surface area, pore volume, and pore size of Fe$_3$O$_4$@SiO$_2$@meso-SiO$_2$-R$_1$ bearing amine functional group are 365 (m^2/g), 0.51 (cm^3/g), and 9.9 (nm), respectively. However Fe$_3$O$_4$@SiO$_2$@meso-SiO$_2$-R$_2$ contains amine functional group has surface area, pore volume, and pore size of 474 (m^2/g), 0.64 (cm^3/g), and 2.1 (nm), respectively. The maximum adsorption capacity of Fe$_3$O$_4$@SiO$_2$@meso-SiO$_2$-R$_1$-NH$_2$ to remove Pb(II), Cd(II), and Cu(II) is 880, 492.4, and 628.3 mg/g. Fe$_3$O$_4$@SiO$_2$@meso-SiO$_2$-R$_2$-NH$_2$ show maximum adsorption capacity, 289.7, 154.2, and 196.5 mg/g for Pb(II), Cd(II), and Cu(II). Fe$_3$O$_4$@SiO$_2$@meso-SiO$_2$-R$_1$-NH$_2$ showed higher adsorption capacity than Fe$_3$O$_4$@SiO$_2$@meso-SiO$_2$-R$_2$-NH$_2$ due to more amine group grated to Fe$_3$O$_4$@SiO$_2$@meso-SiO$_2$-R$_1$-NH$_2$ and other explanation parameter of maximum adsorption mechanism are Langmuir and Freundlich isotherm equation. Basis on value of correlation coefficients (R^2) fitted in Langmuir isotherm equation for Pb(II), Cu(II), and Cd(II) is 0.990, 0.996, and 0.990, respectively; however according to Freundlich isotherm equation correlation coefficients (R^2) value for Pb(II), Cu(II), and Cd(II) are 0.898, 0.922, and 0.940, respectively. The Langmuir experimental data are most suitable and proved that those active sites are distributed in homogeneous fashion to Fe$_3$O$_4$@SiO$_2$@meso-SiO$_2$-R$_1$-NH$_2$ microspheres that showed good adsorption capacity after recycling five times. Thiol functionalized magnetic mesoporous silica nanoparticles are prepared and demonstrated for the heavy metals such as Hg and Pb [129]. The pore diameter, BET surface area, and pore volume and maximum adsorption capacity as fitted with Langmuir isotherm are summarized in Table 4. The removal efficiency and effect of pH have also been investigated. The binding efficiency with meso-SiO$_2$@Fe$_3$O$_4$-SH is Ag(I) $\approx$ Hg(II) > Pb(II) > Cu(II). The increase in pH enhanced the adsorption capacity also. They were employed for the

removal of heavy metals from the natural water resources. The removal efficiency of heavy metals such as Pb, Ag, and Hg is more than 95% while for copper not more than 80%. Low efficiency of copper is due to weak bind to thiol group. It is stable in various natural water in extreme acidic and basic condition. The saturation magnetization of SiO$_2$@ Fe$_3$O$_4$-SH is 38.4 emu/g. The super paramagnetism nature of help to remove adsorbent in the presence of external magnetic field. The removal efficiency was tested with Hg(II). The result showed that more than 90% of Hg(II) is removed after repeated six times magnetic γ-Fe$_2$O$_3$ nanoparticles embedded on the ordered mesoporous carbon (CMK-3) with high surface area which is applicable as magnetic adsorbent to remove toxic chromium(VI) [130].

7. Conclusion

Application of iron oxide nanoparticles based novel magnetic materials for removal of heavy metals from the aqueous systems developed as high efficient and cost-effective nanoadsorbent. Surface modification approach enhanced their stability and efficiency in the water. Magnetic nanoparticles possess an important magnetic property which helps to remove easily in the presence of magnetic field. The reuse of magnetic nanoadsorbent will decrease economic burden. Magnetic nanoadsorbent technology for water remediation is the more convenient and appropriate for removing and separating heavy metals. Before their bulk application health effect and fate into environment of magnetic base nanomaterial should be addressed.

Abbreviations

AF: Amine functionalize
AEMA: Aminoethyl methacrylate
APS: 3-Aminopropyltriethoxy silane
APTMS: Aminotrimethoxysilane
ATRP: Atom transfer radical polymerization
CNTs: Carbon nanotubes
CMβCD: Carboxymethyl-β-cyclodextrin
CTAB: Cetrimethyl ammonium bromide
CS: Chitosan
CCMNPs: Chitosan-coated magnetic nanoparticles
DMSA: Dimercaptosuc cinicacid
DTC: dithiocarbamate,
EDA: ethylenediamine,
EDTA: Ethylenediaminetetraacetic
FA: Foli acid

GMA: Glycidyl methyl acrylate
GA: Gum arabic
HA: Humic acid
INOPs: Iron oxide nanaparticles
KA: Ketoglutaric acid
MNP: Magnetic nanoparticle
MNPs: Magnetic nanaparticles
MBT: 2-Mercaptobenzothiazole
MSA: Mercaptosuccinic
NHS: N-Hydroxy succinimide
PAA: Polyacrylic acid
PCL: Polycaprolactone
PEG: Polyethylene glycol
PEGMA: Polyethylene glycol methacrylate
PEI: Polyethylenimine
PMA: Polymethacrylate
PPy: Polypyrrol
SA: Succinic acid
SPI-NOs: Super paramagnetic iron oxides nanoparticles
USEPA: United States Environment Protection Agency.

Conflict of Interests

The authors declare that there is no conflict of interests regarding the publication of this paper.
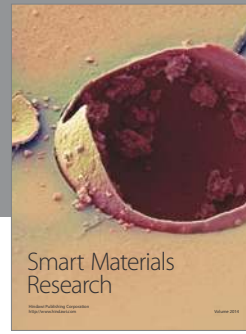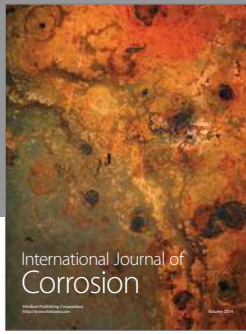
References

[1] R. P. Schwarzenbach, T. Egli, T. B. Hofstetter, U. Von Gunten, and B. Wehrli, "Global water pollution and human health," *Annual Review of Environment and Resources*, vol. 35, pp. 109–136, 2010.

[2] M. Fujita, Y. lde, D. Sato et al., "Heavy metal contamination of coastal lagoon sediments: fongafale islet, Funafuti atoll, tuvalu," *Chemosphere*, vol. 95, pp. 628–634, 2014.

[3] S. K. Al-Musharsfi, I. Y. Mahmoud, and S. N. Al-Bahry, "Heavy metal pollution from treated sewage effluent," *APCBEE Procedia*, vol. 5, pp. 344–348, 2013.

[4] H. A. Naser, "Assessment and management of heavy metal pollution in the marine environment of the Arabian Gulf, a review," *Marine Pollution Bulletin*, vol. 72, no. 1, pp. 6–13, 2013.

[5] G. Akinci, D. E. Guven, and S. K. Ugurlu, "Assessing pollution in Izmir Bay from rivers in western Turkey: heavy metals," *Environmental Science*, vol. 15, no. 12, pp. 2252–2262, 2013.

[6] F. Zan, S. Huo, B. Xi et al., "A 100 year sedimentary record of heavy metal pollution in a shallow eutrophic lake, Lake Chaohu, China," *Journal of Environmental Monitoring*, vol. 13, no. 10, pp. 2788–2797, 2011.

[7] S.-L. Wang, X.-R. Xu, Y.-X. Sun, J.-L. Liu, and H.-B. Li, "Heavy metal pollution in coastal of South China: a review," *Marine Pollution Bulletin*, vol. 76, no. 1-2, pp. 7–15, 2013.

[8] Z. Li, Z. Ma, T. J. D. Kuijp, Z. Yuan, and L. Huang, "A review of soil heavy metal pollution from mines in China: pollution and health risk assessment," *Science of The Total Environment*, vol. 468-469, pp. 843–853, 2014.

[9] S. S. Gowd, M. R. Reddy, and P. K. Govil, "Assessment of heavy metal contamination in soils at Jajmau (Kanpur) and Unnao industrial areas of the Ganga Plain, Uttar Pradesh, India," *Journal of Hazardous Materials*, vol. 174, no. 1–3, pp. 113–121, 2010.

[10] P. C. Deshpande, A. K. Tilwankar, and S. R. Asolekar, "A novel approach to estimating potential maximum exposure to ship recycling yard workers in Alang," *Science of the Total Environment*, vol. 438, pp. 304–311, 2012.

[11] F. Fu and Q. Wang, "Removal of heavy metal ions from wastewaters: a review," *Journal of Environmental Management*, vol. 92, no. 3, pp. 407–418, 2011.

[12] M. A. Hashim, S. Mukhopadhyay, J. N. Sahu, and B. Sengupta, "Remediation technologies for heavy metal contaminated groundwater," *Journal of Environmental Management*, vol. 92, no. 10, pp. 2355–2388, 2011.

[13] L. Zhang and M. Fang, "Nanomaterials in pollution trace detection and environmental improvement," *Nano Today*, vol. 5, no. 2, pp. 128–142, 2010.

[14] M. Hua, S. Zhang, B. Pan, W. Zhang, L. Lv, and Q. Zhang, "Heavy metal removal from water/wastewater by nanosized metal oxides: a review," *Journal of Hazardous Materials*, vol. 211-212, pp. 317–331, 2012.

[15] B. I. Kharisov, H. V. R. Dias, O. V. Kharissova, V. M. Jiménez-Pérez, B. O. Pérez, and B. M. Flores, "Iron-contain nanomaterial: synthesis, properties, and environmental applications," *RSC Advances*, vol. 2, no. 25, pp. 9325–9358.

[16] Z. Feng, S. Zhu, D. R. M. De Godoi, A. C. S. Samia, and D. Scherson, "Adsorption of Cd^{2+} on carboxyl-terminated superparamagnetic iron oxide nanoparticles," *Analytical Chemistry*, vol. 84, no. 8, pp. 3764–3770, 2012.

[17] P. Xu, G. M. Zeng, D. L. Huang et al., "Use of iron oxide nanomaterials in wastewater treatment: a review," *Science of the Total Environment*, vol. 424, pp. 1–10, 2012.

[18] C. L. Warner, W. Chouyyok, K. E. Mackie et al., "Manganese doping of magnetic iron oxide nanoparticles: tailoring surface reactivity for a regenerable heavy metal sorbent," *Langmuir*, vol. 28, no. 8, pp. 3931–3937, 2012.

[19] A. E. Karatapanis, D. E. Petrakis, and C. D. Stalikas, "A layered magnetic iron/iron oxide nanoscavenger for the analytical enrichment of ng-L-1 concentration levels of heavy metals from water," *Analytica Chimica Acta*, vol. 726, pp. 22–27, 2012.

[20] H. Yang, Z. Tian, J. Wang, and S. Yang, "A magnetic resonance imaging nanosensor for Hg (II) based on thymidine-functionalized supermagnetic iron oxide nanoparticles," *Sensors and Actuators B*, vol. 161, no. 1, pp. 429–433, 2012.

[21] A. S. Teja and P.-Y. Koh, "Synthesis, properties, and applications of magnetic iron oxide nanoparticles," *Progress in Crystal Growth and Characterization of Materials*, vol. 55, no. 1-2, pp. 22–45, 2009.

[22] Z. Liu, H. Wang, C. Liu et al., "Magnetic cellulose-chitosan hydrogels prepared from ionic liquids as reusable adsorbent for removal of heavy metal ions," *Chemical Communications*, vol. 48, no. 59, pp. 7350–7352, 2012.

[23] J. K. Oh and J. M. Park, "Iron oxide-based superparamagnetic polymeric nanomaterials: design, preparation, and biomedical application," *Progress in Polymer Science*, vol. 36, no. 1, pp. 168–189, 2011.

[24] S. Laurent, D. Forge, M. Port et al., "Magnetic iron oxide nanoparticles: synthesis, stabilization, vectorization, physicochemical characterizations and biological applications," *Chemical Reviews*, vol. 108, no. 6, pp. 2064–2110, 2008.

[25] L. H. Reddy, J. L. Arias, J. Nicolas, and P. Couvreur, "Magnetic nanoparticles: design and characterization, toxicity and

biocompatibility,pharmaceutical and biomedical applications," *Chemical Reviews*, vol. 112, no. 11, pp. 5818–5878, 2012.

[26] M. Mahmoudi, S. Sant, B. Wang, S. Laurent, and T. Sen, "Superparamagnetic iron oxide nanoparticles (SPIONs): development, surface modification and applications in chemotherapy," *Advanced Drug Delivery Reviews*, vol. 63, no. 1-2, pp. 24–46, 2011.

[27] K. Petcharoen and A. Sirivat, "Synthesis and characterization of magnetite nanoparticles via the chemical co-precipitation method," *Materials Science and Engineering B*, vol. 177, no. 5, pp. 421–427, 2012.

[28] T. Hyeon, S. S. Lee, J. Park, Y. Chung, and B. N. Hyon, "Synthesis of highly crystalline and monodisperse maghemite nanocrystallites without a size-selection process," *Journal of the American Chemical Society*, vol. 123, no. 51, pp. 12798–12801, 2001.

[29] S. Belaid, S. Laurent, M. Vermeersch, L. V. Elst, D. P. Morga, and R. N. Muller, "A new approach to follow the formation of iron oxide nanoparticles synthesized by thermal decomposition," *Nanotechnology*, vol. 24, no. 5.

[30] Y.-H. Zheng, Y. Cheng, F. Bao, and Y.-S. Wang, "Synthesis and magnetic properties of Fe_3O_4 nanoparticles," *Materials Research Bulletin*, vol. 41, no. 3, pp. 525–529, 2006.

[31] B. Behdadfar, A. Kermanpur, H. Sadeghi-Aliabadi, M. D. P. Morales, and M. Mozaffari, "Synthesis of high intrinsic loss power aqueous ferrofluids of iron oxide nanoparticles by citric acid-assisted hydrothermal-reduction route," *Journal of Solid State Chemistry*, vol. 187, pp. 20–26, 2012.

[32] H. Cai, X. An, J. Cui et al., "Facile hydrothermal synthesis and surface functionalization of polyethyleneimine-coated iron oxide nanoparticlesfor biomedical applications," *ACS Applied Materials & Interfaces*, vol. 5, no. 5, pp. 1722–1731, 2013.

[33] S. Cui, X. Shen, and B. Lin, "Surface organic modification of Fe_3O_4 nanoparticles by silane-coupling agents," *Rare Metals*, vol. 25, no. 6, pp. 426–430, 2006.

[34] H. Mohammad-Beigi, S. Yaghmaei, R. Roostaazad, H. Bardania, and A. Arpanaei, "Effect of pH, citrate treatment and silane-coupling agent concentration on the magnetic, structural and surface properties of functionalized silica-coated iron oxide nanocomposite particles," *Physica E*, vol. 44, no. 3, pp. 618–627, 2011.

[35] S. Kango, S. Kalia, A. Celli, J. Njuguna, Y. Habibi, and R. Kumar, "Surface modification of inorganic nanoparticles for development of organic-inorganic nanocomposites," *Progress in Polymer Science*, vol. 38, no. 8, pp. 1232–1261, 20.

[36] C. Barrera, A. P. Herrera, N. Bezares et al., "Effect of poly(ethylene oxide)-silane graft molecular weight on the colloidal properties of iron oxide nanoparticles for biomedical applications," *Journal of Colloid and Interface Science*, vol. 377, no. 1, pp. 40–50, 2012.

[37] E. K. U. Larsen, T. Nielsen, T. Wittenborn et al., "Size-dependent accumulation of pegylated silane-coated magnetic iron oxide nanoparticles in murine tumors," *ACS Nano*, vol. 3, no. 7, pp. 1947–1951, 2009.

[38] F. . Ahangaran, A. Hassanzadeh, and S. Nouril, "Surface modification of $Fe_3O_4@SiO_2$ microsphere by silane coupling agent," *International Nano Letters*, vol. 233, no. 23, pp. 1–5.

[39] D. Forge, S. Laurent, Y. Gossuin, A. Roch, L. Vander Elst, and R. N. Muller, "An original route to stabilize and functionalize magnetite nanoparticles for theranosis applications," *Journal of Magnetism and Magnetic Materials*, vol. 323, no. 5, pp. 410–415, 2011.

[40] J. I. Cutler, D. Zheng, X. Xu, D. A. Giljohann, and C. A. Mirkin, "Polyvalent oligonucleotide iron oxide nanoparticle "click" conjugates," *Nano Letters*, vol. 10, no. 4, pp. 1477–1480, 2010.

[41] C. Huang, K. G. Neoh, and E.-T. Kang, "Combined ATRP and 'click' chemistry for designing stable tumor-targeting superparamagnetic iron oxide nanoparticles," *Langmuir*, vol. 28, no. 1, pp. 563–571, 2012.

[42] C. Huang, K. G. Neoh, and E.-T. Kang, "Combined ATRP and 'click' chemistry for designing stable tumor-targeting superparamagnetic iron oxide nanoparticles," *Langmuir*, vol. 28, no. 1, pp. 563–571, 2012.

[43] C. Huang, K. G. Neoh, L. Xu, E. T. Kang, and E. Chiong, "Polymeric nanoparticles with encapsulated superparamagnetic iron oxide and conjugated cisplatin for potential bladder cancer therapy," *Biomacromolecules*, vol. 13, no. 8, pp. 2513–2520, 2012.

[44] L. Wang, K. G. Neoh, E. T. kang, and B. Shuter, "Methotrexate-conjugated and hyperbranched polyglycerol-grafted Fe_3O_4 magnetic nanoparticles for targeted anticancer effects," *European Journal of Pharmaceutical Sciences*, vol. 48, no. 1-2, pp. 111–120, 2013.

[45] J. Vidal-Vidal, J. Rivas, and M. A. López-Quintela, "Synthesis of monodisperse maghemite nanoparticles by the microemulsion method," *Colloids and Surfaces A*, vol. 288, no. 1–3, pp. 44–51, 2006.

[46] A. B. Chin and I. I. Yaacob, "Synthesis and characterization of magnetic iron oxide nanoparticles via w/o microemulsion and Massart's procedure," *Journal of Materials Processing Technology*, vol. 191, no. 1–3, pp. 235–237, 2007.

[47] L.-H. Han, H. Liu, and Y. Wei, "In situ synthesis of hematite nanoparticles using a low-temperature microemulsion method," *Powder Technology*, vol. 207, no. 1–3, pp. 42–46, 2011.

[48] R. J. Joseyphus, D. Kodama, T. Matsumoto, Y. Sato, B. Jeyadevan, and K. Tohji, "Role of polyol in the synthesis of Fe particles," *Journal of Magnetism and Magnetic Materials*, vol. 310, no. 2, pp. 2393–2395, 2007.

[49] W. Cai and J. Wan, "Facile synthesis of superparamagnetic magnetite nanoparticles in liquid polyols," *Journal of Colloid and Interface Science*, vol. 305, no. 2, pp. 366–370, 2007.

[50] M. Abbas, B. P. Rao, S. M. Naga, M. Takahashi, and C. G. Kim, "Synthesis of high magnetization hydrophilic magnetite (Fe_3O_4) nanoparticles in single reaction-surfactntless polyol process," *Ceramics International*, vol. 39, no. 7, pp. 7605–7611, 2013.

[51] R. Abu Mukh-Qasem and A. Gedanken, "Sonochemical synthesis of stable hydrosol of Fe_3O_4 nanoparticles," *Journal of Colloid and Interface Science*, vol. 284, no. 2, pp. 489–494, 2005.

[52] S.-J. Park, S. Kim, S. Lee, Z. G. Khim, K. Char, and T. Hyeon, "Synthesis and magnetic studies of uniform iron nanorods and nanospheres," *Journal of the American Chemical Society*, vol. 122, no. 35, pp. 8581–8582, 2000.

[53] E. H. Kim, H. S. Lee, B. K. Kwak, and B.-K. Kim, "Synthesis of ferrofluid with magnetic nanoparticles by sonochemical method for MRI contrast agent," *Journal of Magnetism and Magnetic Materials*, vol. 289, pp. 328–330, 2005.

[54] B. M. Kumfer, K. Shinoda, B. Jeyadevan, and I. M. Kennedy, "Gas-phase flame synthesis and properties of magnetic iron oxide nanoparticles with reduced oxidation state," *Journal of Aerosol Science*, vol. 41, no. 3, pp. 257–265, 2010.

[55] Y. Li, Y. Hu, G. Huang, and C. Li, "Metallic iron nanoparticles: flame synthesis, characterization and magnetic properties," *Particuology*, vol. 11, no. 4, pp. 460–467, 2013.

[56] R. W. Saunders and J. M. C. Plane, "The formation and growth of Fe_2O_3 nanoparticles from the photo-oxidation of iron pentacarbonyl," *Journal of Aerosol Science*, vol. 41, no. 5, pp. 475–489, 2010.

[57] H. Cui, Y. Liu, and W. Ren, "Structure switch between α-Fe_2O_3, γ-Fe_2O_3 and Fe_3O_4 during the large scale and low temperature sol-gel synthesis of nearly monodispersed iron oxide nanoparticles," *Advanced Powder Technology*, vol. 24, no. 1, pp. 93–97, 2013.

[58] R. F. C. Marques, C. Garcia, P. Lecante et al., "Electro-precipitation of Fe_3O_4 nanoparticles in ethanol," *Journal of Magnetism and Magnetic Materials*, vol. 320, no. 19, pp. 2311–2315, 2008.

[59] L. Cabrera, S. Gutierrez, N. Menendez, M. P. Morales, and P. Herrasti, "Magnetite nanoparticles: electrochemical synthesis and characterization," *Electrochimica Acta*, vol. 53, no. 8, pp. 3436–3441, 2008.

[60] F. Fajaroh, H. Setyawan, W. Widiyastuti, and S. Winardi, "Synthesis of magnetite nanoparticles by surfactant-free electrochemical method in an aqueous system," *Advanced Powder Technology*, vol. 23, no. 3, pp. 328–333, 2012.

[61] S. Lin, D. Lu, and Z. Lu, "Removal of arsenic contaminants with magnetic γ-Fe_2O_3 nanoparticles," *Chemical Engineering*, vol. 211-212, pp. 46–52, 2012.

[62] S. Luther, N. Borgfeld, J. Kim, and J. G. Parsons, "Removal of arsenic from aqueous solution: a study of the effects of pH and interfering ions using iron oxide nanomaterials," *Microchemical Journal*, vol. 101, pp. 30–36, 2012.

[63] W. Tang, Q. Li, S. Gao, and J. K. Shang, "Arsenic (III,V) removal from aqueous solution by ultrafine α-Fe_2O_3 nanoparticles synthesized from solvent thermal method," *Journal of Hazardous Materials*, vol. 192, no. 1, pp. 131–138, 2011.

[64] M. Kilianova, R. Prucek, J. Filip et al., "Remarkable efficiency of ultrafine superparamagnetic iron (III) oxide nanoparticles toward arsenate removal from aqueous environment," *Chemosphere*, vol. 93, no. 11, pp. 2690–2697, 2013.

[65] K. Song, W. Kim, C.-Y. Suh, D. Shin, K.-S. Ko, and K. Ha, "Magnetic iron oxide nanoparticles prepared by electrical wire explosion for arsenic removal," *Powder Technology*, vol. 246, pp. 572–574, 2013.

[66] M. Kokate, K. Garadkar, and A. Gole, "One pot synthesis of magnetite-silica nanocomposites: applications as tags, entrapment matrix and in water purification," *Journal of Materials Chemistry A*, vol. 1, no. 6, pp. 2022–2029, 2013.

[67] S. Zhang, H. Niu, Y. Cai, X. Zhao, and Y. Shi, "Arsenite and arsenate adsorption on coprecipitated bimetal oxide magnetic nanomaterials: $MnFe_2O_4$ and $CoFe_2O_4$," *Chemical Engineering Journal*, vol. 158, no. 3, pp. 599–607, 2010.

[68] V. Chandra, J. Park, Y. Chun, J. W. Lee, I.-C. Hwang, and K. S. Kim, "Water-dispersible magnetite-reduced graphene oxide composites for arsenic removal," *ACS Nano*, vol. 4, no. 7, pp. 3979–3986, 2010.

[69] I. F. Nata, M. Sureshkumar, and C.-K. Lee, "One-pot preparation of amine-rich magnetite/bacterial cellulose nanocomposite and its application for arsenate removal," *RSC Advances*, vol. 1, no. 4, pp. 625–631, 2011.

[70] Z. Wu, W. Li, P. A. Webley, and D. Zhao, "General and controllable synthesis of novel mesoporous magnetic iron oxide@carbon encapsulates for efficient arsenic removal," *Advanced Materials*, vol. 24, no. 4, pp. 485–491, 2012.

[71] R. M. Dhoble, S. Lunge, A. G. Bhole, and S. Rayalu, "Magnetic binary oxide particles (MBOP): a promising adsorbent for removal of As (III) in water," *Water Research*, vol. 45, no. 16, pp. 4769–4781, 2011.

[72] Y. Tian, M. Wu, X. Lin, P. Huang, and Y. Huang, "Synthesis of magnetic wheat straw for arsenic adsorption," *Journal of Hazardous Materials*, vol. 193, pp. 10–16, 2011.

[73] J. Ma, Z. Zhu, B. Chen et al., "One-pot, large-scale synthesis of magnetic activated carbon nanotubes and their applications for arsenic removal," *Journal of Materials Chemistry A*, vol. 1, no. 15, pp. 4662–4666, 2013.

[74] B. K. Mandal and K. T. Suzuki, "Arsenic round the world: a review," *Talanta*, vol. 58, no. 1, pp. 201–235, 2002.

[75] B. An, Q. Liang, and D. Zhao, "Removal of arsenic(V) from spent ion exchange brine using a new class of starch-bridged magnetite nanoparticles," *Water Research*, vol. 45, no. 5, pp. 1961–1972, 2011.

[76] Arsenic in drinking water, http://water.epa.gov/lawsregs/rules-regs/sdwa/arsenic/index.cfm.

[77] W. Yang, A. T. Kan, W. Chen, and M. B. Tomson, "PH-dependent effect of zinc on arsenic adsorption to magnetite nanoparticles," *Water Research*, vol. 44, no. 19, pp. 5693–5701, 2010.

[78] C. T. Yavuz, J. T. Mayo, C. Suchecki et al., "Pollution magnet: nano-magnetite for arsenic removal from drinking water," *Environmental Geochemistry and Health*, vol. 32, no. 4, pp. 327–334, 2010.

[79] Y. Jeong, M. Fan, S. Singh, C.-L. Chuang, B. Saha, and J. Hans van Leeuwen, "Evaluation of iron oxide and aluminum oxide as potential arsenic(V) adsorbents," *Chemical Engineering and Processing*, vol. 46, no. 10, pp. 1030–1039, 2007.

[80] L. Feng, M. Cao, X. Ma, Y. Zhu, and C. Hu, "Superparamagnetic high-surface-area Fe_3O_4 nanoparticles as adsorbents for arsenic removal," *Journal of Hazardous Materials*, vol. 217-218, pp. 439–446, 2012.

[81] X. Yu, S. Tong, M. Ge, J. Zuo, C. Cao, and W. Song, "One-step synthesis of magnetic composites of cellulose@iron oxide nanoparticles for arsenic removal," *Journal of Materials Chemistry A*, vol. 1, no. 3, pp. 959–965, 2013.

[82] R. Chalasani and S. Vasudevan, "Cyclodextrin functionalized magnetic iron oxide nanocrystal: a host-carrier for magnetic separation of non-polar molecules and arsenic from aqueous media," *Journal of Materials Chemistry*, vol. 22, pp. 14925–14931, 2012.

[83] F. Mou, J. Guan, Z. Xiao, Z. Sun, W. Shi, and X.-A. Fan, "Solvent-mediated synthesis of magnetic Fe_2O_3 chestnut-like amorphous-core/γ-phase-shell hierarchical nanostructures with strong As(v) removal capability," *Journal of Materials Chemistry*, vol. 21, no. 14, pp. 5414–5421, 2011.

[84] Y.-M. Hao, C. Man, and Z.-B. Hu, "Effective removal of Cu (II) ions from aqueous solution by amino-functionalized magnetic nanoparticles," *Journal of Hazardous Materials*, vol. 184, no. 1–3, pp. 392–399, 2010.

[85] H. Li, D.-L. Xiao, H. He, R. Lin, and P.-L. Zuo, "Adsorption behavior and adsorption mechanism of Cu (II) ions on amino-functionalized magnetic nanoparticles," *Transactions of Nonferrous Metals Society of China*, vol. 23, no. 9, pp. 2657–2665, 2013.

[86] S. S. Banerjee and D.-H. Chen, "Fast removal of copper ions by gum arabic modified magnetic nano-adsorbent," *Journal of Hazardous Materials*, vol. 147, no. 3, pp. 792–799, 2007.

[87] Y.-T. Zhou, H.-L. Nie, C. Branford-White, Z.-Y. He, and L.-M. Zhu, "Removal of Cu^{2+} from aqueous solution by chitosan-coated magnetic nanoparticles modified with α-ketoglutaric

acid," *Journal of Colloid and Interface Science*, vol. 330, no. 1, pp. 29–37, 2009.

[88] Y.-C. Chang and D.-H. Chen, "Preparation and adsorption properties of monodisperse chitosan-bound Fe_3O_4 magnetic nanoparticles for removal of Cu(II) ions," *Journal of Colloid and Interface Science*, vol. 283, no. 2, pp. 446–451, 2005.

[89] H. Yan, L. Yang, Z. Yang, H. Yang, A. Li, and R. Cheng, "Preparation of chitosan/poly (acrylic acid) magnetic composite microspheres and applications in the removal of copper (II) ions from aqueous solutions," *Journal of Hazardous Materials*, vol. 229-230, pp. 371–380, 2012.

[90] J.-Y. Tseng, C.-Y. Chang, C.-F. Chang et al., "Kinetics and equilibrium of desorption removal of copper from magnetic polymer adsorbent," *Journal of Hazardous Materials*, vol. 171, no. 1–3, pp. 370–377, 2009.

[91] A. Z. M. Badruddoza, A. S. H. Tay, P. Y. Tan, K. Hidajat, and M. S. Uddin, "Carboxymethyl-β-cyclodextrin conjugated magnetic nanoparticles as nano-adsorbents for removal of copper ions: synthesis and adsorption studies," *Journal of Hazardous Materials*, vol. 185, no. 2-3, pp. 1177–1186, 2011.

[92] J. Zhu, S. Wei, H. Gu et al., "One-pot synthesis of magnetic graphene nanocomposites decorated with core@double-shell nanoparticles for fast chromium removal," *Environmental Science and Technology*, vol. 46, no. 2, pp. 977–985, 2012.

[93] P. Yuan, M. Fan, D. Yang et al., "Montmorillonite-supported magnetite nanoparticles for the removal of hexavalent chromium [Cr(VI)] from aqueous solutions," *Journal of Hazardous Materials*, vol. 166, no. 2-3, pp. 821–829, 2009.

[94] G. López-Téllez, C. E. Barrera-Díaz, P. Balderas-Hernández, G. Roa-Morales, and B. Bilyeu, "Removal of hexavalent chromium in aquatic solutions by iron nanoparticles embedded in orange peel pith," *Chemical Engineering Journal*, vol. 173, no. 2, pp. 480–485, 2011.

[95] Y. Wang, B. Zou, T. Gao, X. Wu, S. Lou, and S. Zhou, "Synthesis of orange-like Fe_3O_4/PPy composite microspheres and their excellent Cr(VI) ion removal properties," *Journal of Materials Chemistry*, vol. 22, no. 18, pp. 9034–9040, 2012.

[96] N. N. Nassar, "Rapid removal and recovery of Pb(II) from wastewater by magnetic nanoadsorbents," *Journal of Hazardous Materials*, vol. 184, no. 1–3, pp. 538–546, 2010.

[97] Z. Cheng, A. L. KuanTan, Y. Tao, D. Shan, K. E. Ting, and X. J. Yin, "Synthesis and characterization of iron Oxide nanoparticles and applications in the removal of heavy Metals from industrial wastewater," *International Journal of Photoenergy*, vol. 2012, pp. 1–5, 2012.

[98] P. Xu, G. M. Zeng, D. L. Huang et al., "Adsorption of Pb (II) by iron oxide nanoparticles immobilized phanerochaete chrysosporium: equilibrium, kinetic, thermodynamic and mechanisms analysis," *Chemical Engineering Journal*, vol. 203, pp. 423–431, 2012.

[99] T. Madrakian, A. Afkhami, and M. Ahmadi, "Simple *in situ* functionalizing magnetite nanoparticles by reactive blue-19 and their application to the effective removal of Pb^{2+} ions from water samples," *Chemosphere*, vol. 90, no. 2, pp. 542–547, 2013.

[100] L. Wang, J. Li, Q. Jiang, and L. Zhao, "Water-soluble Fe_3O_4 nanoparticles with high solubility for removal of heavy-metal ions from waste water," *Dalton Transactions*, vol. 41, no. 15, pp. 4544–4551, 2012.

[101] C.-Y. Cao, J. Qu, W.-S. Yan, J.-F. Zhu, Z.-Y. Wu, and W.-G. Song, "Low-cost synthesis of flowerlike α-Fe_2O_3 nanostructures for heavy metal ion removal: adsorption property and mechanism," *Langmuir*, vol. 28, no. 9, pp. 4573–4579, 2012.

[102] Z. Wei, R. Xing, X. Zhang, S. Liu, H. Yu, and P. Li, "Facile template-free fabrication of hollow nestlike α-Fe_2O_3 nanostructures for water treatment," *ACS Applied Materials & Interfaces*, vol. 5, no. 3, pp. 598–604, 2013.

[103] A. Roy and J. Bhattacharya, "Removal of Cu (II), Zn (II) and Pb (II) from water using microwave-assisted synthesized maghemite nanotubes," *Chemical Engineering Journal*, vol. 211-212, pp. 493–500, 2012.

[104] C. Zhang, J. Sui, J. Li, Y. Tang, and W. Cai, "Efficient removal of heavy metal ions by thiol-functionalized super magnetic carbon nanotubes," *Chemical Engineering Journal*, vol. 210, pp. 45–52, 2012.

[105] H. Parham, B. Zargar, and R. Shiralipour, "Fast and efficient removal of mercury from water samples using magnetic iron oxide nanoparticles modified with 2-mercaptobenzothiazole," *Journal of Hazardous Materials*, vol. 205-206, pp. 94–100, 2012.

[106] X. Xin, Q. Wei, J. Yang et al., "Highly efficient removal of heavy metal ions by amine-functionalized mesoporous Fe_3O_4 nanoparticles," *Chemical Engineering Journal*, vol. 184, pp. 132–140, 2012.

[107] F. Ge, M.-M. Li, H. Ye, and B.-X. Zhao, "Effective removal of heavy metal ions Cd^{2+}, Zn^{2+}, Pb^{2+}, Cu^{2+} from aqueous solution by polymer-modified magnetic nanoparticles," *Journal of Hazardous Materials*, vol. 211-212, pp. 366–372, 2012.

[108] J.-F. Liu, Z.-S. Zhao, and G.-B. Jiang, "Coating Fe_3O_4 magnetic nanoparticles with humic acid for high efficient removal of heavy metals in water," *Environmental Science and Technology*, vol. 42, no. 18, pp. 6949–6954, 2008.

[109] S. Singh, K. C. Barick, and D. Bahadur, "Surface engineered magnetic nanoparticles for removal of toxic metal ions and bacterial pathogens," *Journal of Hazardous Materials*, vol. 192, no. 3, pp. 1539–1547, 2011.

[110] A. Z. M. Badruddoza, Z. B. Shawon, W. J. Tay, K. Hidajat, and M. S. Uddin, "Fe_3O_4/cyclodextrin polymer nanocomposites for selective heavy metals from industrial wastewater," *Carbohydrate Polymers*, vol. 91, no. 1, pp. 322–332, 2013.

[111] J. Gong, L. Chen, G. Zeng et al., "Shellac-coated ironoxide nanaparticles for removal of cadmium (II) ions from aqueous solution," *Journal of Environmental Sciences*, vol. 24, no. 7, pp. 1165–1173, 2012.

[112] W. Yantasee, C. L. Warner, T. Sangvanich et al., "Removal of heavy metals from aqueous systems with thiol functionalized superparamagnetic nanoparticles," *Environmental Science and Technology*, vol. 41, no. 14, pp. 5114–5119, 2007.

[113] Y. Tan, M. Chen, and Y. Hao, "High efficient removal of Pb (II) by amino-functionalized Fe_3O_4 magnetic nano-particles," *Chemical Engineering Journal*, vol. 191, pp. 104–111, 2012.

[114] Y. F. Shen, J. Tang, Z. H. Nie, Y. D. Wang, Y. Ren, and L. Zuo, "Preparation and application of magnetic Fe_3O_4 nanoparticles for wastewater purification," *Separation and Purification Technology*, vol. 68, no. 3, pp. 312–319, 2009.

[115] F. Zhang, Z. Zhu, Z. Dong et al., "Magnetically recoverable facile nanomaterials: synthesis, characterization and application in remediation of heavy metals," *Microchemical Journal*, vol. 98, no. 2, pp. 328–333, 2011.

[116] A. Farrukh, A. Akram, A. Ghaffar et al., "Design of polymer-brush grafted magnetic nanaparticles for highly efficient water remediation," *Mater Interfaces*, vol. 5, no. 9, pp. 3784–3793, 2013.

[117] S. Yang, Z. Guo, G. Sheng, and X. Wang, "Application of novel plasma-induced CD/MWCNT/ iron oxide composite in zinc decontamination," *Carbohydrate Polymers*, vol. 90, no. 2, pp. 1100–1105, 2012.

[118] E.-J. Kim, C.-S. Lee, Y.-Y. Chang, and Y.-S. Chang, "Hierarchically structured manganese oxide -caoted magnetic nanocomposites for the efficient removal of heavy metal ions from aqueous systems," *ACS Applied Materials & Interfaces*, vol. 19, no. 5, pp. 9628–9634, 2013.

[119] S. Singh, K. C. Barick, and D. Bahadur, "Fe_3O_4 embedded Zno nanocomposites for the removal of toxic metal ions organic dyes and bacterial pathogens," *Journal of Materials Chemistry A*, vol. 1, no. 10, pp. 3325–3333, 2013.

[120] Z. Ma, D. Zhao, Y. Chang, S. Xing, Y. Wu, and Y. Gao, "Synthesis of $MnFe_2O_4$@Mn-Co oxide core-shell nanaparticles and their excellent performance for heavy metal removal," *Dalton Transactions*, vol. 42, no. 39, pp. 14261–14267, 2013.

[121] S.-H. Huang and D.-H. Chen, "Rapid removal of heavy metal cations and anions from aqueous solutions by an amino-functionalized magnetic nano-adsorbent," *Journal of Hazardous Materials*, vol. 163, no. 1, pp. 174–179, 2009.

[122] A. R. Mahdavian and M. A.-S. Mirrahimi, "Efficient separation of heavy metal cations by anchoring polyacrylic acid on superparamagnetic magnetite nanoparticles through surface modification," *Chemical Engineering Journal*, vol. 159, no. 1–3, pp. 264–271, 2010.

[123] H. Karami, "Heavy metal removal from water by magnetite nanorods," *Chemical Engineering Journal*, vol. 219, pp. 209–216, 2013.

[124] A. E. Karatapanis, Y. Fiamegos, and C. D. Stalikas, "Silica-modified magnetic nanoparticles functionalized with cetylpyridinium bromide for the preconcentration of metals after complexation with 8-hydroxyquinoline," *Talanta*, vol. 84, no. 3, pp. 834–839, 2011.

[125] C. Caparrós, M. Benelmekki, P. M. Martins et al., "Hydrothermal assisted synthesis of iron oxide-based magnetic silica spheres and their performance in magnetophoretic water purification," *Chemical Physics*, vol. 135, pp. 510–517, 2012.

[126] J. Wang, S. Zheng, Y. Shao, J. Liu, Z. Xu, and D. Zhu, "Amino-functionalized Fe_3O_4@SiO_2 core-shell magnetic nanomaterial as a novel adsorbent for aqueous heavy metals removal," *Journal of Colloid and Interface Science*, vol. 349, no. 1, pp. 293–299, 2010.

[127] S. Zhang, Y. Zhang, J. Liu et al., "Thiol modified Fe_3O_4@SiO_2 as a robust ,high effective and recycling magnetic sorbent for mercury removal," *Chemical Engineering Journal*, vol. 226, pp. 30–38, 2013.

[128] Q. Yuan, N. Li, Y. Chi et al., "Effect of large pore size of multifunctional mesoporous microsphere on removal of heavy metal ions," *Journal of Hazardous Materials*, vol. 254-255, pp. 157–165, 2013.

[129] G. Li, Z. Zhao, J. Liu, and G. Jiang, "Effective heavy metal removal from aqueous systems by thiol functionalized magnetic mesoporous silica," *Journal of Hazardous Materials*, vol. 192, no. 1, pp. 277–283, 2011.

[130] M. Baikousi, A. B. Bourlinos, A. Douvalis et al., "Synthesis and characterization of γ-Fe_2O_3/carbon hybrids and their application in removal of hexavalent chromium ions from aqueous solutions," *Langmuir*, vol. 28, no. 8, pp. 3918–3930, 2012.

Journal of
Nanotechnology

International Journal of
Corrosion

International Journal of
Polymer Science

Smart Materials
Research

Journal of
Composites

BioMed
Research International

Journal of
Metallurgy

Journal of
Materials

Submit your manuscripts at
http://www.hindawi.com

Journal of
Nanoparticles

Advances in
Materials Science and Engineering

Scientifica

Journal of
Nanomaterials

The Scientific World Journal

International Journal of
Biomaterials

Journal of
Nanoscience

Journal of
Coatings

Journal of
Crystallography

Journal of
Ceramics

Journal of
Textiles